EXTENDED ARRAY EVALUATION PROGRAM. SPECIAL REPORT NO. 16. PRELIMINARY COMPARISON OF AUTOMATIC FISHER AND CONVENTIONAL POWER DETECTION ALGORITHMS

Stephen S. Lane

Texas Instruments, Incorporated

Prepared for:

Advanced Research Projects Agency
Air Force Technical Applications Center

30 November 1973

UNCLASSIFIED
Security Classification

AD 783 608

DOCUMENT CONTROL DATA - R & D

(Security classification of title, body of abstract and indexing annotation must be entered when the overall report is classified)

1 ORIGINATING ACTIVITY (Corporate author)
Texas Instruments Incorporated
Equipment Group
Dallas, Texas 75222

2a. REPORT SECURITY CLASSIFICATION
UNCLASSIFIED

2b. GROUP

3 REPORT TITLE
Preliminary Comparison of Automatic Fisher and Conventional Power Detection Algorithms, Special Report No. 16

4 DESCRIPTIVE NOTES (Type of report and inclusive dates)
Special

5 AUTHOR(S) (First name, middle initial, last name)
Stephen S. Lane

6 REPORT DATE
30 November 1973

7a. TOTAL NO OF PAGES
~~38~~ 40

7b. NO OF REFS
4

8a. CONTRACT OR GRANT NO
Contract No. F33657-72-C-0725

b PROJECT NO
AFTAC Project No.
VELA T/2705/B/ASD

c.

d.

9a. ORIGINATOR'S REPORT NUMBER(S)
ALEX(01)-STR-73-16

9b OTHER REPORT NO(S) (Any other numbers that may be assigned this report)

10 DISTRIBUTION STATEMENT
APPROVED FOR PUBLIC RELEASE, DISTRIBUTION UNLIMITED

11 SUPPLEMENTARY NOTES
ARPA Order No. 1714

12 SPONSORING MILITARY ACTIVITY
Advanced Research Projects Agency
Nuclear Monitoring Research Office
Arlington, Virginia 22209

13 ABSTRACT

The performance of two seismic event detectors, the Fisher detector and the conventional power detector, was compared. Long-period records with low signal-to-noise ratios, recorded at the Alaskan Long Period Array, were used to establish performance characteristics, sensitivities, response to off-azimuth events, and response to signal distortion. Results confirmed the theoretical prediction that there is no important distinction between the detectors.

40

DD FORM 1 NOV 68 1473

UNCLASSIFIED
Security Classification

14 KEY WORDS	LINK A		LINK B		LINK C	
	ROLE	WT	ROLE	WT	ROLE	WT
Automatic Detection						
Fisher Detector						
False Alarm Rate						
Detection Probability						

ALEX(01)-STR-73-16

PRELIMINARY COMPARISON OF AUTOMATIC FISHER AND CONVENTIONAL POWER DETECTION ALGORITHMS

SPECIAL REPORT NO. 16

EXTENDED ARRAY EVALUATION PROGRAM

Prepared by
Stephen S. Lane

TEXAS INSTRUMENTS INCORPORATED
Equipment Group
Post Office Box 6015
Dallas, Texas 75222

Prepared for

AIR FORCE TECHNICAL APPLICATIONS CENTER
AFTAC Project No. VELA T/2705/B/ASD
Alexandria, Virginia 22314

Sponsored by

ADVANCED RESEARCH PROJECTS AGENCY
Nuclear Monitorining Research Office
ARPA Program Code No. 2F10
ARPA Order No. 1714

30 November 1973

Acknowledgment: This research was supported by the Advanced Research Projects Agency, Nuclear Monitoring Research Office under Project VELA-UNIFORM, and accomplished under the technical direction of the Air Force Technical Applications Center under Contract No. F33657-72-C-0725.

ABSTRACT

The performance of two seismic event detectors, the Fisher detector and the conventional power detector, was compared. Long-period records with low signal-to-noise ratios, recorded at the Alaskan Long Period Array, were used to establish performance characteristics, sensitivities, response to off-azimuth events, and response to signal distortion. Results confirmed the theoretical prediction that there is no important distinction between the detectors.

TABLE OF CONTENTS

SECTION	TITLE	PAGE
	ABSTRACT	iii
I.	INTRODUCTION	I-1
II.	DESCRIPTION OF THE FISHER DETECTOR	II-1
III.	ANALYSIS OF THE DATA	III-1
	A. FALSE ALARM RATE, PROBABILITY OF DETECTION, AND THE PERFORMANCE CHARACTERISTIC	III-1
	B. RESPONSE TO OFF-AZIMUTH SIGNALS	III-11
	C. RESPONSE TO DISTORTED SIGNALS	III-14
	D. RESPONSE TO SIGNAL IRREGULARITIES	III-14
IV.	CONCLUSIONS	IV-1
V.	REFERENCES	V-1
	APPENDIX A	A-1

LIST OF FIGURES

FIGURE	TITLE	PAGE
III-1	PROGRAM OUTPUT FOR 15 BEAM DIRECTIONS AND TWO TIME GATES	III-2
III-2	PROBABILITY OF DETECTION FOR FISHER AND CONVENTIONAL DETECTOR AT 32 SECOND TIME GATE	III-7
III-3	FALSE ALARM RATE FOR FISHER AND CONVENTIONAL DETECTORS AT 32 SECOND TIME GATE	III-8
III-4	PERFORMANCE CHARACTERISTICS FOR FISHER DETECTOR	III-10
III-5	PERFORMANCE CHARACTERISTICS FOR FISHER AND CONVENTIONAL DETECTORS WITH 256 SECOND TIME GATE	III-12
III-6	AZIMUTHAL RESPONSE OF FISHER AND CONVENTIONAL DETECTORS FOR 256 SECOND TIME GATE	III-13
III-7	FISHER AND CONVENTIONAL DETECTOR RESPONSE	III-15
III-8	RESPONSE OF FISHER AND CONVENTIONAL DETECTORS TO GLITCH IN DATA	III-16

LIST OF TABLES

TABLE	TITLE	PAGE
III-1	EVENTS STUDIED	III-5
III-2	LEVEL SPACING	III-6

SECTION I
INTRODUCTION

This report studies the performance of two seismic signal detectors; the Fisher detector, (Edwards, Benno, and Creasey, 1967), and the beam power detector. These detectors are designed to automatically process seismic data and alert the analyst whenever some criterion is met which indicates the presence of a signal. The Fisher detector responds to similarities among the outputs of the array elements, while the power detector responds to sudden changes in the average power level over the array.

This report investigates the response of the detectors to signals of varying signal-to-noise ratio; their performance characteristics in terms of false alarm rate versus detection probability; their response to off-azimuth signals; and their response to irregularities in the data such as glitches, spikes, and amplitude and phase distortion. Both theoretical and experimental results are presented.

SECTION II
DESCRIPTION OF THE FISHER DETECTOR

The Fisher detector is an algorithm which responds to similarities in the time-delayed traces from an array of identically oriented seismometers. Time-delaying the traces has the effect of forming a beam in the direction specified by the delay times. A time averaging feature is included so that signal similarity must persist for some time before the detector responds. Thus brief accidental similarity due to noise will be suppressed. Incoherent noise is dissimilar from one site to another, whereas propagating signals are similar. Therefore, the detector will respond to propagating signals of sufficiently great duration.

The Fisher detector takes advantage of the fact that the mean square of a series of numbers is the same as the squared mean only when the numbers are identically the same. The numbers in this case are the time shifted outputs of M seismometers. If $y_i(t) = x_i(t-\tau_i)$ where x_i is the output of the i-th seismometer at the time t, and τ_i is time shift required to form a particular beam, the detector calculates the quantity:

$$\frac{1}{M}\sum_{i=1}^{M} y_i^2(t) - \left\{\frac{1}{M}\sum_{i=1}^{M} y_i(t)\right\}^2 \qquad (1)$$

The Fisher detector is the inverse of (1), normalized by multiplying by $(M-1)\left\{\frac{1}{M}\sum_{i=1}^{M} y_i(t)\right\}^2$. A time average of the sums formed is taken, before the detector output is formed. Then the detector output is:

$$S(t) = \frac{(M-1)\overline{\left\{\frac{1}{M}\sum_{i=1}^{M} y_i\right\}^2}}{\frac{1}{M}\sum_{i=1}^{M} y_i^2 - \overline{\left\{\frac{1}{M}\sum_{i=1}^{M} y_i\right\}^2}} \qquad (2)$$

where the bar denotes averaging over some time before the output time t. If the seismometer outputs are all the same the Fisher output increases without limit. For real signals with noise the seismometer outputs are not exactly the same, and the Fisher output reaches some finite value as shown below for a few special cases.

Equation 2 has the form

$$S(t) = \frac{(M-1)\ \overline{B^2}}{\frac{1}{M}\sum_{i=1}^{M} y_i^2 - \overline{B^2}} \qquad (3)$$

where B is the ordinary beam output i.e.,

$$B(t) = \frac{1}{M}\sum_{i=1}^{M} y_i(t) \qquad (4)$$

The conventional beam power detector is:

$$P(t) = \frac{1}{\sigma_o^2}\ \overline{B^2} \qquad (5)$$

where σ_o is the mean square value of the noise preceding the signal at a single site.

To find the sensitivity of the Fisher and conventional power detectors we assume that the signals of interest are long period and are thus well dispersed. Then the peak amplitude of such a signal will consist of very nearly sinusoidal motion. We therefore consider the response of the detectors to one frequency component of the signals, in the presence of noise.

The amplitude of the signal with wavenumber $\bar{k}$ will be A. The signal amplitude will be assumed constant over the array for the moment. Site positions are denoted by $\bar{X}_j$, and there are M sites. The noise varies from site to site, with amplitude n_j and phase ϕ_j at the j-th site. Then the signal vector is:

$$T = \begin{bmatrix} \cdot \\ \cdot \\ y_j(\bar{k}) \\ \cdot \\ \cdot \\ \cdot \end{bmatrix} = A \begin{bmatrix} \cdot \\ \cdot \\ e^{i\bar{k}\cdot X_j} \\ \cdot \\ \cdot \\ \cdot \end{bmatrix} + \begin{bmatrix} \cdot \\ \cdot \\ n_j e^{i\phi_j} \\ \cdot \\ \cdot \end{bmatrix} \tag{6}$$

and the data matrix is

$$\Omega = TT^H = AA^* \begin{bmatrix} \cdot \\ \cdot \\ e^{i\bar{k}\cdot\bar{X}_j} \\ \cdot \\ \cdot \\ \cdot \end{bmatrix} \begin{bmatrix} \cdot\cdot e^{-i\bar{k}\cdot X_p} \cdots \end{bmatrix} + \begin{bmatrix} \cdot \\ \cdot \\ n_j e^{i\phi_j} \\ \cdot \\ \cdot \end{bmatrix} \begin{bmatrix} \cdot\cdot n_p e^{-i\phi_p} \cdots \end{bmatrix} \tag{7}$$

The noise has been assumed uncorrelated with the signal.

The beam power is obtained from the data matrix by

$$B = L^H TT^H L = AA^* + \frac{1}{M^2} \sum_{j=1}^{M} n_j n_j^* = AA^* + \frac{1}{M}\ \sigma_o^2 \tag{8}$$

where $L(\bar{p})$ is the look direction vector, and $\bar{p} = \bar{k}$.

$$L(\bar{p}) = \frac{1}{M} \begin{bmatrix} \cdot \\ \cdot \\ e^{i\bar{p}\cdot\bar{X}_n} \\ \cdot \\ \cdot \\ \cdot \end{bmatrix} \tag{9}$$

The beam power detector output is then:

$$\frac{AA^* + \frac{1}{M}\sigma_o^2}{\frac{1}{M}\sigma_o^2} = 1 + M\frac{AA^*}{\sigma_o^2} \tag{10}$$

Inserting these results in equation 3 for the Fisher detector

$$S = \frac{(M-1)\left(AA^* + \frac{1}{M}\sigma_o^2\right)}{\frac{1}{M}\sum_{j=1}^{M}\left(A + n_j e^{i\phi_j}\right)^2 - AA^* - \frac{1}{M}\sigma_o^2} \tag{11}$$

Cross terms between the signal and noise in the sum of squares average to zero, and 11 reduces to

$$S = \frac{(M-1)\left(AA^* + \frac{1}{M}\sigma_o^2\right)}{\sigma_o^2\left(1 - \frac{1}{M}\right)} \tag{12}$$

Assuming $M>>1$, this is

$$1 + M\frac{AA^*}{\sigma_o^2} \tag{13}$$

just as for the beam power detector.

To find the response of the beam power detector to an off-azimuth signal we make $\bar{p}$ different from $\bar{k}$ in equations 6 and 9. The result is

$$P = \frac{AA^*}{M^2}\left[\sum_{j=1}^{M} e^{i(\bar{k} - \bar{p}) \cdot X_j}\right]^2 + \frac{1}{M}\ \sigma_o^2 \qquad (14)$$

The first term is the array response and is a function of the array coordinates. Its maximum occurs when $\bar{k} = \bar{p}$.

If we denote the quantity called the array response in 14 by $\alpha(\bar{p})$

$$\alpha(\bar{p}) = \frac{1}{M^2}\left\{\sum_{j=1}^{M} e^{i(\bar{k} - \bar{p}) \cdot X_j}\right\}^2 \qquad (15)$$

and rewrite the expression 11 for the Fisher detector in the presence of an off-azimuth signal, we find

$$S = \frac{(M-1)\left(AA^*\ \alpha(\bar{p}) + \frac{1}{M}\ \sigma_o^2\right)}{AA^*\ (1 - \alpha(\bar{p})) + \sigma_o^2\ (1 - \frac{1}{M})} \qquad (16)$$

Both the Fisher detector and the beam power detector have their maximum when the look direction coincides with the signal wave vector. It will be shown below that as the look direction moves from the signal azimuth, the first minimum in their outputs occurs at the same change in azimuth. Therefore their resolutions are the same.

The derivative of 16 with respect to the look direction vector $\bar{p}$ is

$$\frac{dS}{d\bar{p}} = \frac{(M-1)\ AA^*\left\{AA^*\ (1-\alpha) + \sigma_o^2(1 - \frac{1}{M})\right\} + AA^*\left\{AA^*\alpha + \frac{1}{M}\ \sigma_o^2\right\}}{\left\{AA^*\ (1-\alpha) + \sigma_o^2\ (1 - \frac{1}{M})\right\}^2} \qquad (17)$$

and this is zero only when $d\alpha/d\bar{p}$, the derivative of the array response with respect to look direction, is zero. But the beam power detector's derivative with respect to angle is

$$\frac{dp}{d\bar{p}} = \frac{AA^*}{\sigma_o^2} \quad \frac{d\alpha}{d\bar{p}} \tag{18}$$

and this is zero at the same point.

Next we consider the effect of irregularities in the data. Such irregularities may be random, such as glitches or spikes, or systematic, such as variations in response from one seismometer to another.

When a glitch or spike is present we can no longer use signal vectors to represent the data. These irregularities may be thought of as large, roughly constant deviations from the mean at one seismometer. They differ from one another in their time duration - spikes are short and glitches are long. In either case the seismometers outputs will no longer be similar to one another, and the Fisher detector's output should go to that expected for uncorrelated noise.

We will represent a glitch as a site whose amplitude is constant at G over the time averaging interval. Using 4 for the beam output we have in this case.

$$B^2(t) = \left\{ \frac{1}{M} \sum_{j=1}^{M-1} y_j(t) + \frac{G}{M} \right\}^2 \tag{19}$$

Carrying out the squaring gives

$$B^2(t) = \left\{ \frac{1}{M} \sum_{j=1}^{M-1} y_j(t) \right\}^2 + \frac{2G}{M} \left\{ \frac{1}{M} \sum_{j=1}^{M-1} y_j(t) \right\} + \frac{G^2}{M^2} \tag{20}$$

When the time average is taken the cross term between the glitch and the rest of the seismometers goes to zero.

The first term may be represented (almost) as a beam formed from M-1 seismometers, differing from that quantity only by a factor of (M-1)/M. For large M this will make no important difference. Thus the beam power output is

$$B^2(t) = B^2_{M-1}(t) + \frac{G^2}{M^2} \tag{21}$$

where B^2_{M-1} is the "reduced" beam. Thus we can conclude that the beam power detector will always be larger in the presence of a glitch than in its absence, whether a signal is present or not.

Next we insert these results into equation 3 for the Fisher detector

$$S(t) = \frac{(M-1)\left(\overline{B^2_{M-1}} + \frac{G^2}{M^2}\right)}{\frac{1}{M}\sum_{j=1}^{\overline{M-1}} y_j^2 - \overline{B^2_{M-1}} + \frac{G^2}{M}\left(1 - \frac{1}{M}\right)} \tag{22}$$

It can be seen that this output is almost the same as that without the glitch, except that $(M-1)\,G^2/M^2$ has been added to the numerator, and $\frac{G^2}{M}\left(1-\frac{1}{M}\right)$ to the denominator. A little algebraic manipulation shows that this always has the effect of reducing the output. The limit for G very large is 1, as expected.

Spikes may be treated in very much the way glitches are, except that since they are of short duration they have much less effect on the output.

Next suppose that the response to a plane wave varies from station to station, whether due to variations in siesmometers or geology. The signal vector is

$$T = \begin{bmatrix} \vdots \\ A_j e^{i(\phi_j + \bar{k} \cdot \bar{x}_j)} + n_j \\ \vdots \end{bmatrix} \tag{23}$$

where the A_j's and the ϕ_j's differ from site to site. Then the beam power is

$$B = \frac{1}{M^2} \sum_{j=1}^{M} \sum_{k=1}^{M} \left\{ A_j A_k^* e^{i(\phi_j - \phi_k)} - n_j n_k^* \right\} \tag{24}$$

Defining $\bar{A} = \frac{1}{M} \sum_{j=1}^{M} A_j$ and $\delta_j = A_j - \bar{A}$ we have

$$B = \frac{1}{M^2} \sum_{j=1}^{M} \sum_{k=1}^{M} \left\{ \bar{A}\bar{A}^* - \bar{A}\delta_k^* + \bar{A}^* \delta_j + \delta_j \delta_k \right\} e^{i(\phi_j - \phi_k)} - \frac{1}{M} \sigma_o^2 \tag{25}$$

The second sum averages to zero, as do those terms in the third for which $j \neq k$. Defining

$$\alpha^2 = \sum_{j=1}^{M} \sum_{k=1}^{M} e^{i(\phi_j - \phi_k)} \tag{26}$$

and

$$\beta^2 = \frac{1}{\bar{A}\bar{A}^*} \frac{1}{M} \sum_{k=1}^{M} \delta_k \delta_k^* \tag{27}$$

the beam power detector becomes

$$P = 1 + M \frac{\bar{A}\bar{A}^*}{\sigma_o^2} \left(\alpha + \frac{\beta^2}{M} \right) \tag{28}$$

The parameter α^2 is a measure of phase distortion and is near one for a practical array. Amplitude distortion is measured by β^2. Reasonable values for β^2 lie between .01 and .02 at ALPA.

The expression for the Fisher detector is

$$S = \frac{(M-1)\left\{\bar{A}\bar{A}^*(\alpha^2 + \frac{\beta^2}{M}) + \frac{1}{M}\sigma_o^2\right\}}{\frac{1}{M}\sum_{k=1}^{M}\overline{\left(A_j e^{i\phi_j} + n_j\right)^2} - \left\{\bar{A}\bar{A}^*(\alpha^2 + \frac{\beta^2}{M}) + \frac{1}{M}\sigma_o^2\right\}} \tag{29}$$

which becomes after time averaging

$$S = \frac{(M-1)\left\{\bar{A}\bar{A}^*(\alpha^2 + \frac{\beta^2}{M}) + \frac{1}{M}\sigma_o^2\right\}}{\frac{1}{M}\sum_{k=1}^{M}(\bar{A}\bar{A}^* + \bar{A}S_k^* + \bar{A}^*S_k + S_kS_k^*) - \bar{A}\bar{A}^*(\alpha^2 + \frac{\beta^2}{M}) + \frac{1}{M}\sigma_o^2} \tag{30}$$

Averaging over sites as before leads to

$$S = \frac{(M-1)\ \bar{A}\bar{A}^*(\alpha^2 + \frac{\beta^2}{M}) + \frac{1}{M}\sigma_o^2}{\bar{A}\bar{A}^*(1-\alpha^2 + \beta^2(1-\frac{1}{M}) + (1-\frac{1}{M})\sigma_o^2} \tag{31}$$

From these expressions it can be seen that the beam power output increases indefinately as the signal amplitude increases, but that the Fisher detector saturates at a level dependent on the kind and degree of distortion present. For pure phase distortion, the Fisher detector output can go no higher than $\frac{(M-1)\alpha^2}{1-\alpha^2}$. If only amplitude distortion is present, it is limited to the value

$$\frac{(M-1)(\frac{\beta^2}{M}+1)}{\beta^2(1-\frac{1}{M})}$$

When both are present, saturation occurs at

$$\frac{(M-1)\left(\alpha^2+\frac{\beta^2}{M}\right)}{1-\alpha^2+\beta^2\left(1-\frac{1}{M}\right)}$$

SECTION III
ANALYSIS OF THE DATA

The purpose of this section is to test the predictions of Section II with real data, and to evaluate the performance of both detectors in terms of an objective criterion, the performance characteristic. Data used were long-period signals from events in the $3.7 \leq m_b \leq 4.1$ range and long-period noise recorded at the Alaskan Long Period Array (ALPA). Processing used about 13 sites.

A. FALSE ALARM RATE, PROBABILITY OF DETECTION, AND THE PERFORMANCE CHARACTERISTIC

1. Definitions

The program output takes the form shown in Figure III-1. Time, at 32 second intervals, is printed on the left. Next comes a row of symbols, one for each azimuth. These symbols represent the output level of the Fisher detector for the first time gate, at the time in question. The time gate is the interval over which data are averaged in the detector definition. The range of outputs which gives rise to a particular symbol is displayed at the end of the plot, as part of a histogram which gives the number of times each symbol occurred for each time gate and azimuth. Next comes the conventional power detector output levels for the same azimuths, output time, and time gate. The second row gives the Fisher and conventional detector outputs for the same azimuths, but for the next time gate, and so on.

It is anticipated that the detector will run continuously, forming beams which cover all azimuths with some rather small angular spacing. Whenever the output, on a particular beam, exceeds some predetermined test

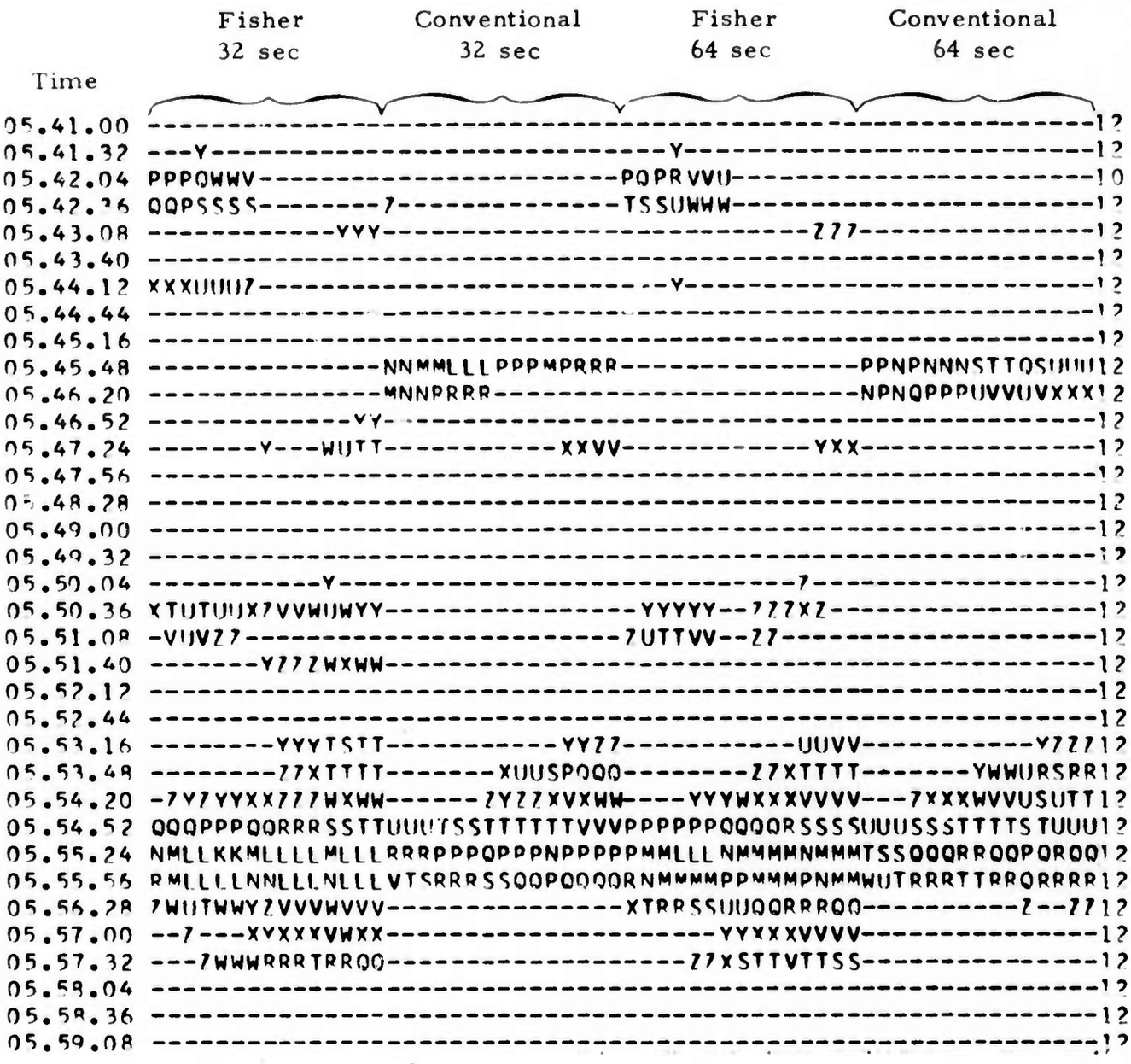

Azimuths Spaced at 15° Intervals Around Primary Beam Direction
Detector Level as in Table III-2

FIGURE III-1

PROGRAM OUTPUT FOR 15 BEAM DIRECTIONS
AND TWO TIME GATES

level, the data are further analyzed to determine whether the output was due to a seismic event, or to some form of noise. The detector will therefore function as a flag, which alerts the analyst to the need for further investigation.

The detector output can reach a given test level by chance, even if the input is noise, and this is called a false alarm. The number of times this happens, per unit time, is the false alarm rate. On the other hand, it may not reach the level required for a detection even with a signal present, if the signal is small or distorted. The probability of reaching a given test level when a signal is present is called the probability of detection for that level. The probability of reaching a given test level is of course either zero or one for a particular event, depending on its signal-to-noise ratio. Nevertheless, an average detection probability, which will tell us how likely it is that some as yet uninvestigated event will trigger the detector, can be estimated.

From a plot such as Figure III-1 for pure noise the false alarm rate for each detector can be calculated as a function of time gate length. The false alarm rate for a given power level is defined as the average number of times, in a standard time interval, that the detector output increases past that level. Any number of consecutive output values which exceed a given level is counted as only one false alarm at that level.

Thus if the detector output increased past the power level represented by J in Figure III-1, four times in a 8192 second noise sample, the false alarm rate for the J-th level would be 4 per 8192 seconds. False alarm rates are normalized to 256 seconds in this report, so here the false alarm rate would be $4/(8192/256) = .125$ per unit time interval.

The performance characteristic is found by eliminating the threshold level between the detection probability and the false alarm rate.

Thus threshold level becomes a parameter in the performance characteristic. That detector is best which, at a fixed false alarm rate, has the highest detection probability.

2. Experimental Procedure

To determine the detection probability, events were processed with both detectors. The highest value for the on-azimuth detector, within the signal arrival gate, was noted. The fraction of the events whose maximum output reached or exceeded a given test level was the probability of detection for that level.

The events studied here are listed in Table III-1, according to bodywave magnitude. It should be noted that they cover a wide range of epicentral distances and are distributed over the region of interest, and that their magnitudes are near the 50% detection level for ALPA (Strauss, 1973). Thus these events form a good sample on which to test the detector's potential for surveillance work.

Figure III-2 shows the probability of detection versus detector level for both conventional and Fisher detectors for the $m_b = 4.1$ events. The Fisher detector shows a lower probability of detection over this range of levels.

A 2 hour 15 minute noise sample recorded on August 26, 1970 was used to determine the false alarm rate. Data were taken for three different beams, so the effective length was 6 hours 45 minutes, corresponding to about 760 averaging periods of 32 seconds each. The false alarm rate, as defined above, is shown in Figure III-3 as a function of test level for both Fisher detector and conventional power detector, at a time gate of 32 seconds. The Fisher detector shows a higher false alarm rate for a given level, but this finding has no significance in terms of performance, until it is combined with the detection probability curve by eliminating the level between Figures III-2 and III-3.

TABLE III-1

EVENTS STUDIED

m_b = 4.1	m_b = 3.9	m_b = 3.7
KUR-171-22AL	IRA-186-09AL	KAM-033-04AL
KAM-032-10AL	TUR-196-04AL	ITY-036-03AL
KAM-059-12AL	BIB-232-04AL	KUR-054-05QC
KUR-235-03AL	KOM-011-08AL	KUR-049-14QC
KAM-063-00AL	KAM-016-11AL	LOM-054-10AL
KUR-228-22AL	KOM-042-13AL	WRS-056-22QC
KAM-192-12AL	IRA-029-09AL	KUR-066-09AL
TIB-037-04AL	CHI-030-03AL	KUR-070-06AL
IRA-041-16QC	CRS-059-15QC	KOR-074-15AL
TIB-073-18AL	KAM-180-14AL	OKH-078-19AL
IRA-154-00AL	KUR-153-00AL	MON-153-11AL
TUR-160-12AL	SIN-154-06AL	TSI-154-16AL
IRA-187-21AL	TIB-195-05AL	KUR-162-19AL
RYU-192-00AL	MED-199-03AL	IIQ-168-23AL
PAK-214-09AL	TIB-202-10AL	ERS-172-09AL
		TUR-175-04QC
		YUG-177-04AL
		HIN-178-20AL
		CKZ-181-00QC
		KAM-197-13AL
		CKZ-200-06AL
		KAM-206-10AL
		RYU-214-05AL
		KUR-231-23AL
		KUR-236-10AL
		KUR-241-09AL
		TIB-242-23AL
		MON-244-17AL

TABLE III-2

LEVEL SPACING

	>	12.3	+
11.8	to	12.3	A
11.3	to	11.8	B
10.9	to	11.3	C
10.4	to	10.9	D
10.0	to	10.4	E
9.5	to	10.0	F
9.1	to	9.5	G
8.6	to	9.1	H
8.2	to	8.6	J
7.8	to	8.2	K
7.4	to	7.8	L
7.0	to	7.4	M
6.6	to	7.0	N
6.2	to	6.6	P
5.8	to	6.2	Q
5.5	to	5.8	R
5.1	to	5.5	S
4.8	to	5.1	T
4.4	to	4.8	U
4.1	to	4.4	V
3.8	to	4.1	W
3.5	to	3.8	X
3.3	to	3.5	Y
3.0	to	3.3	Z
	<	3.0	-

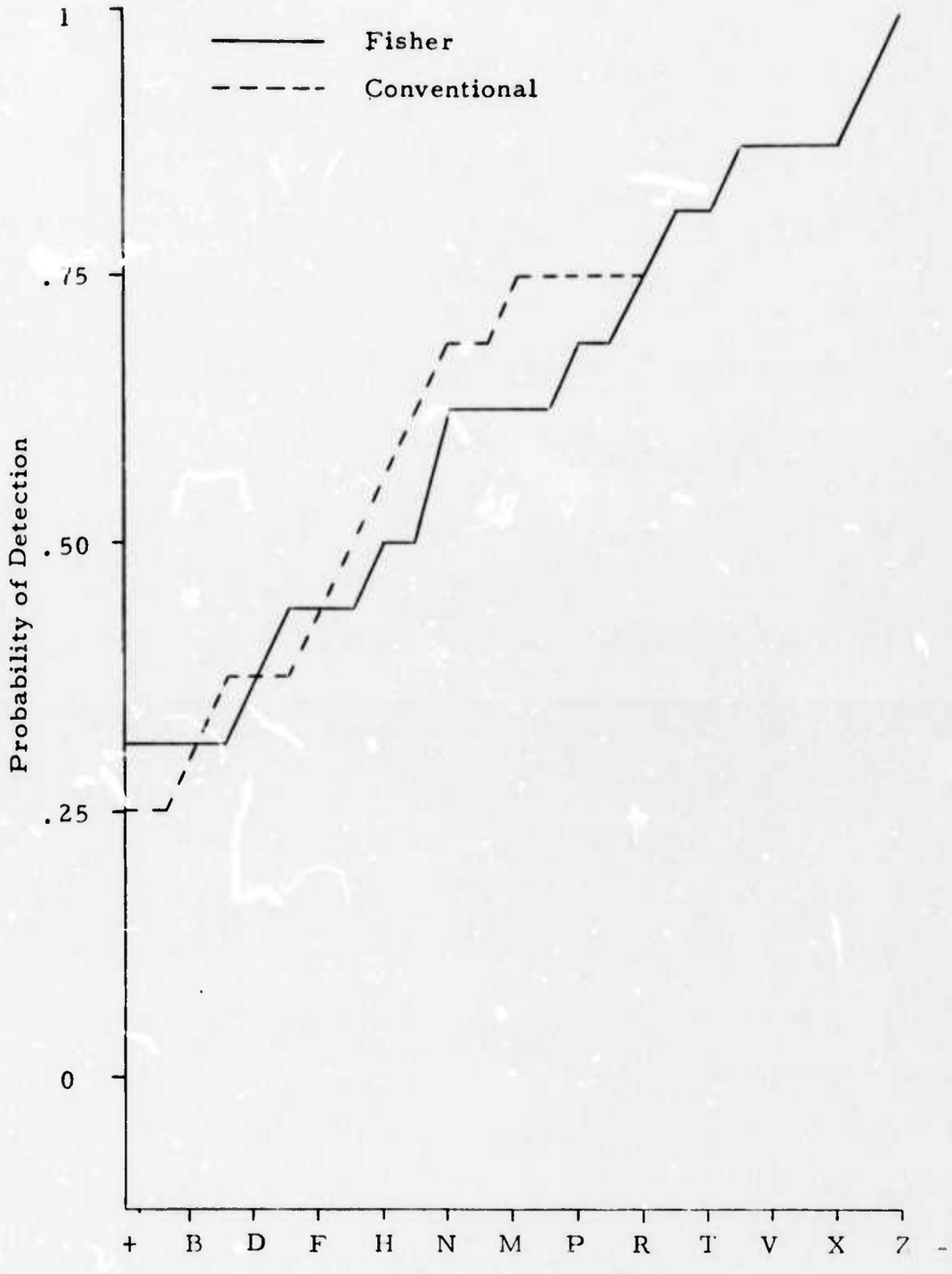

FIGURE III-2

PROBABILITY OF DETECTION FOR FISHER AND CONVENTIONAL DETECTOR AT 32 SECOND TIME GATE

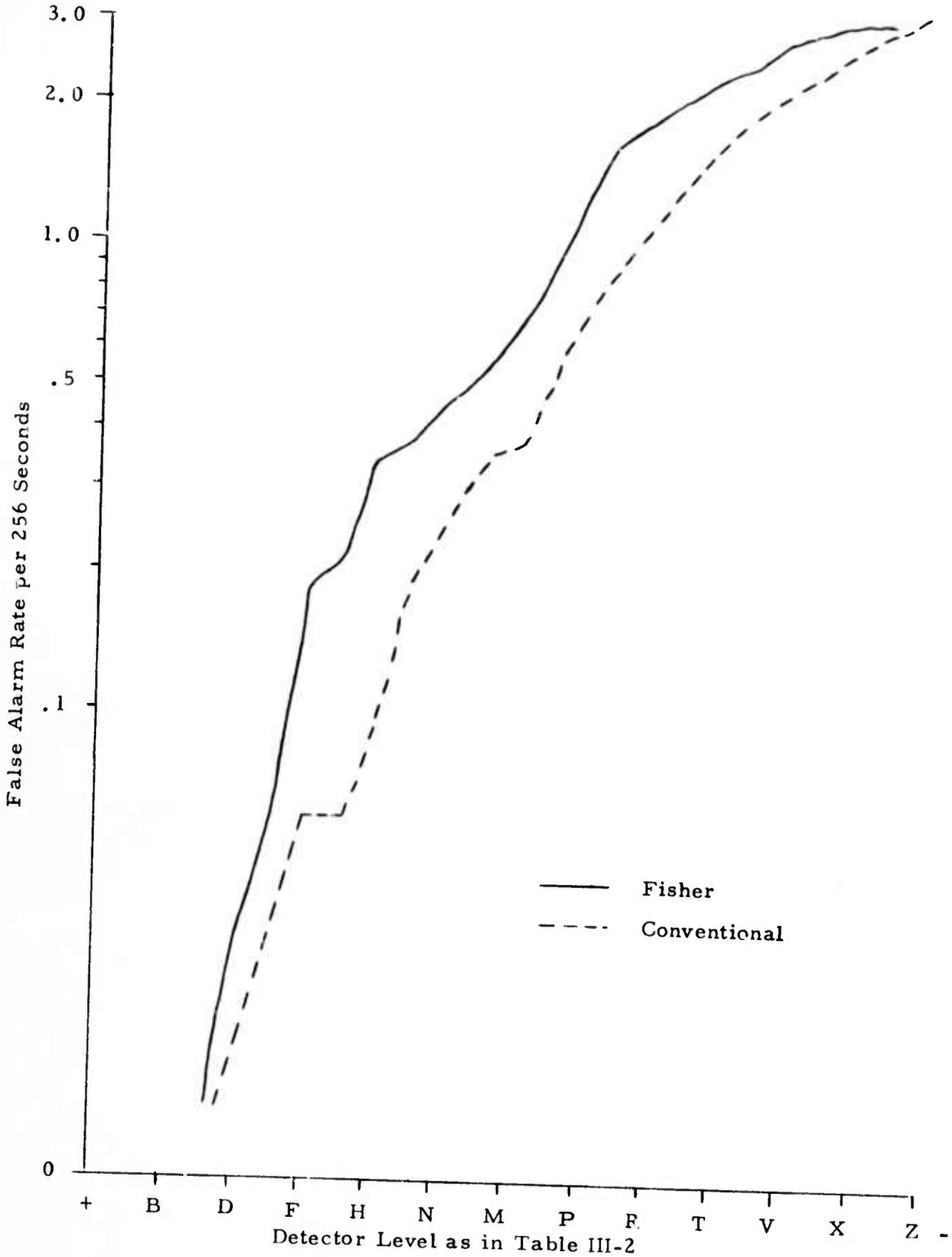

FIGURE III-3

FALSE ALARM RATE FOR FISHER AND CONVENTIONAL DETECTORS AT 32 SECOND TIME GATE

3. Results and Discussion

Performance characteristics for the Fisher detector were calculated separately for events of m_b = 4.1, 3.9, and 3.7. To determine if the performance characteristics differed from magnitude to magnitude, tests on the equality of the probability of a detection at fixed false alarm rates but different magnitudes were performed. It was found, that the difference observed was not significant at the 75% confidence level. The reason for this effect is that events of the same bodywave magnitude have differing signal-to-noise ratios at ALPA due to distance and radiation pattern effects on the signals and temporal variations of the noise. For this reason, all the events studied were lumped together, and the results of this report are valid for m_b near 4.0.

Figure III-4 shows the performance characteristics for the Fisher detector, for time gates of length 32, 64, 128, and 256 seconds. A test on the equality of the probability of detection at a false alarm rate of .2 per 256 seconds shows that the observed deviations between the 32 second gate and the 256 second gate are real at the 85% confidence level.

This confidence level is not as high as one might hope for, and might be increased by taking a larger sample. However, the regular increase in detection probability with gate length at a given false alarm rate is additional evidence that the difference is real. Thus it is concluded that for low signal-to-noise ratio events the detector with a 256 second signal gate is superior to that with a 32 second gate, at false alarm rates of .2 per 256 seconds and lower.

False alarms are due to fluctuations in the mean value of the noise, and the standard deviation of the mean power of uncorrelated noise is proportional to $2/N$, where N is the sample length. Thus increasing the gate length decreases the false alarm rate. On the other hand, signal-to-noise ratio drops off slowly with time gate length so long as the gate length is

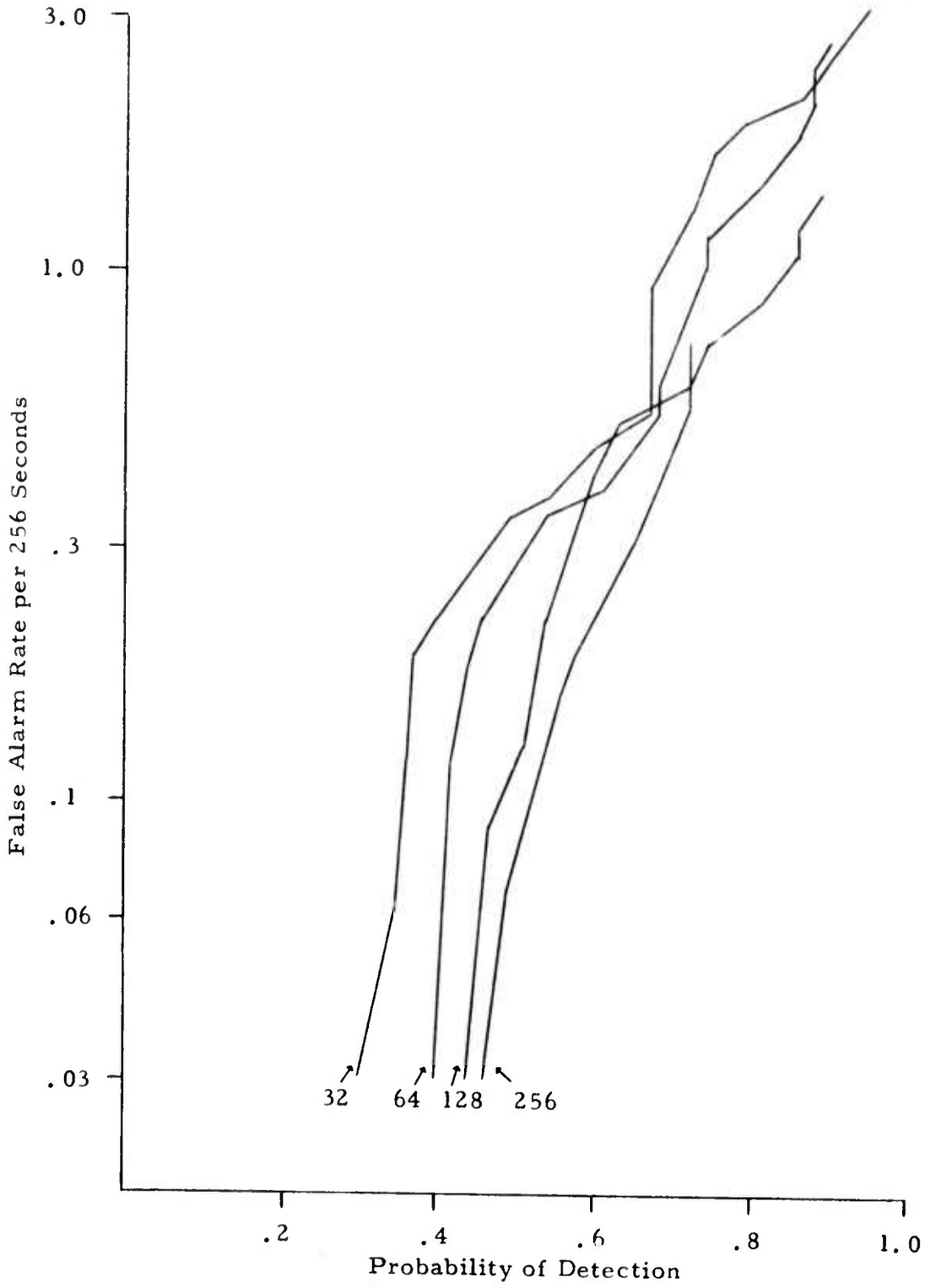

FIGURE III-4

PERFORMANCE CHARACTERISTICS FOR FISHER DETECTOR

less than the signal length. Since the detector responds to signal-to-noise ratio, this means that detection probabilities drop off slowly with time gate length. This explains the observed result, and suggests that still longer gates would give more attractive performance characteristics, up to a point which depends on signal length and thus on magnitude.

At higher false alarm rates this superiority of the larger gate disappears. However, because practical limitations would preclude operating at high false alarm rates, this effect is largely academic. For example, a false alarm rate of .2/256 seconds corresponds to about 3 per hour, which already might be close to the upper limit that the overall detection system could tolerate.

The confidence level for the hypothesis that the other pairs of the four gates examined are different is too low to claim that they are in fact different. However, it is reasonable to assume that the 256 second gate works best, and attention will be restricted to it for the remainder of this report.

Next, in Figure III-5, the conventional and Fisher detectors performance characteristics are compated at a time gate of 256 seconds. The largest deviation, occurring at about .7 false alarms per 256 seconds, is not statistically significant. It is concluded that there is no significant difference in the performance characteristics of the Fisher and conventional detectors for 256 second time gates.

B. RESPONSE TO OFF-AZIMUTH SIGNALS

To find the response of off-azimuth events for each detector, the detector outputs were plotted in Figure III-6 at a fixed time as a function of azimuth for a magnitude 4.1 event. The side lobes of the response are obscured by the noise so the angle at which the detectors reach a minimum is not visible. Rejection of off-azimuth signals is the same over the range studied, as predicted in Section II.

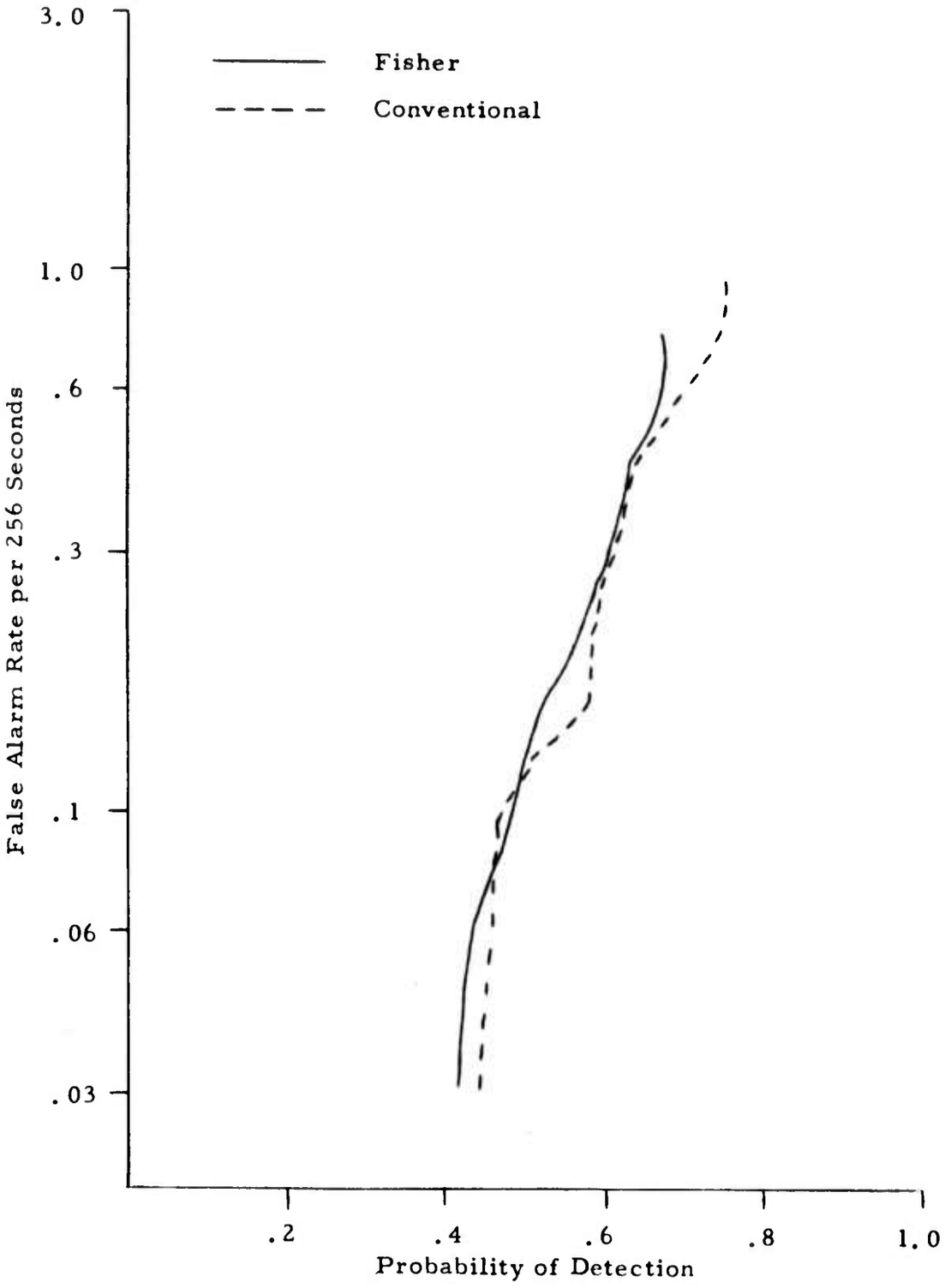

FIGURE III-5

PERFORMANCE CHARACTERISTICS FOR FISHER AND CONVENTIONAL DETECTORS WITH 256 SECOND TIME GATE

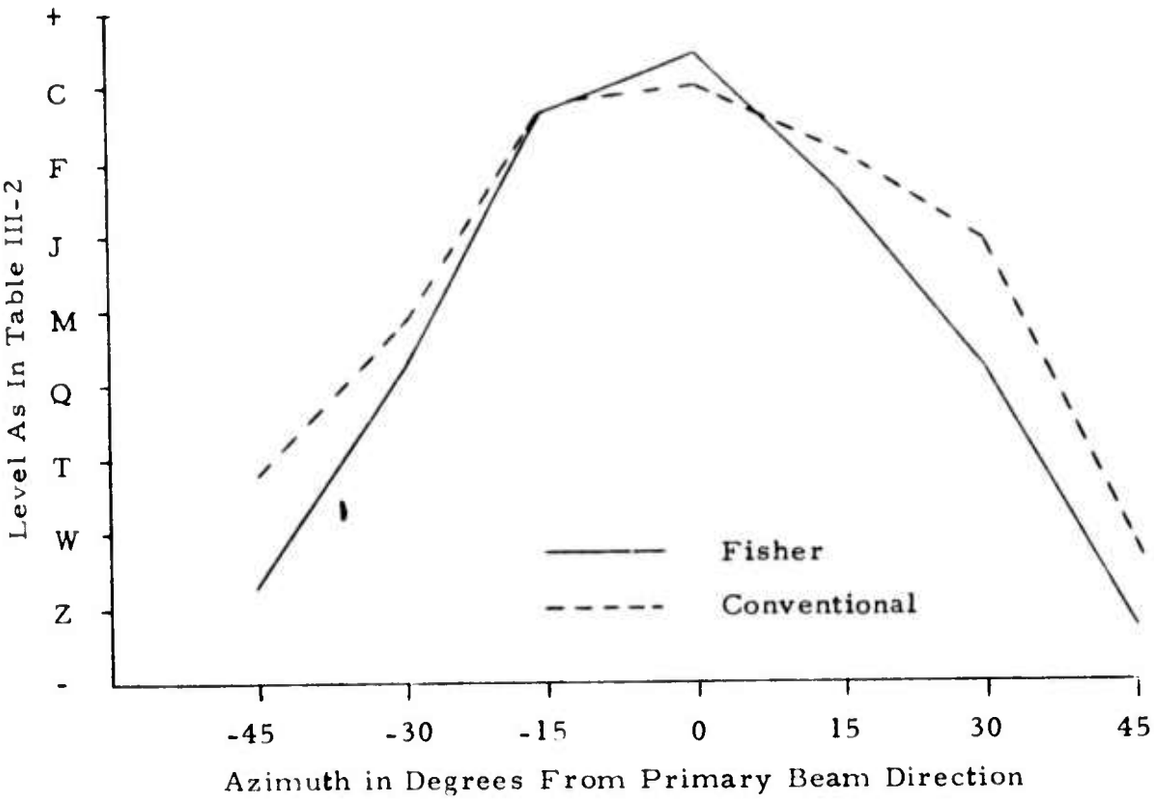

FIGURE III-6

AZIMUTHAL RESPONSE OF FISHER AND CONVENTIONAL DETECTORS FOR 256 SECOND TIME GATE

C. RESPONSE TO DISTORTED SIGNALS

Figure III-7 shows the amplitudes of Fisher and conventional detectors as a function of time for KAM-168-09AL, a magnitude 4.1 event. The output of the Fisher detector falls somewhat below that of the conventional power detector.

Amplitudes for this event were so low that amplitude distortion could not be measured from the individual site time traces. Therefore β^2 was assumed to be .015, a typical value at ALPA. The results of Section II were used to calculate a value of α of .73.

The parameter α corresponds to an average cosine of the phase distortion across the array, and is thus related to an average time delay anomaly. The dominant period of motion for this event was 20 seconds, and this leads to an average time delay anomaly of about 2 seconds. We might expect delay anomalies of half this amount due to the fact that individual sites can be time-aligned only within a sampling period of 2 seconds. Variations of the signal azimuth with time and genuine departures from plane wave propagation presumably can raise the time delay anomalies to 2 seconds.

Such saturation due to phase distortion is no detriment to the detector's utility. For practical arrays where α^2 is near one, saturation will occur at a level well above that at which signals are further investigated. Thus saturation will not change the performance characteristics within the range of reasonable false alarm rates.

D. RESPONSE TO SIGNAL IRREGULARITIES

Figure III-8 shows the result of a large glitch at time 6 hours 35 minutes 24 seconds. The conventional detector reaches a value larger that the upper bin limit, and the fisher detector goes to a value smaller than the smallest bin limit. This is in agreement with the results of Section II, where it was predicted that a glitch would drive the conventional detector to very large values and the Fisher detector to 1.

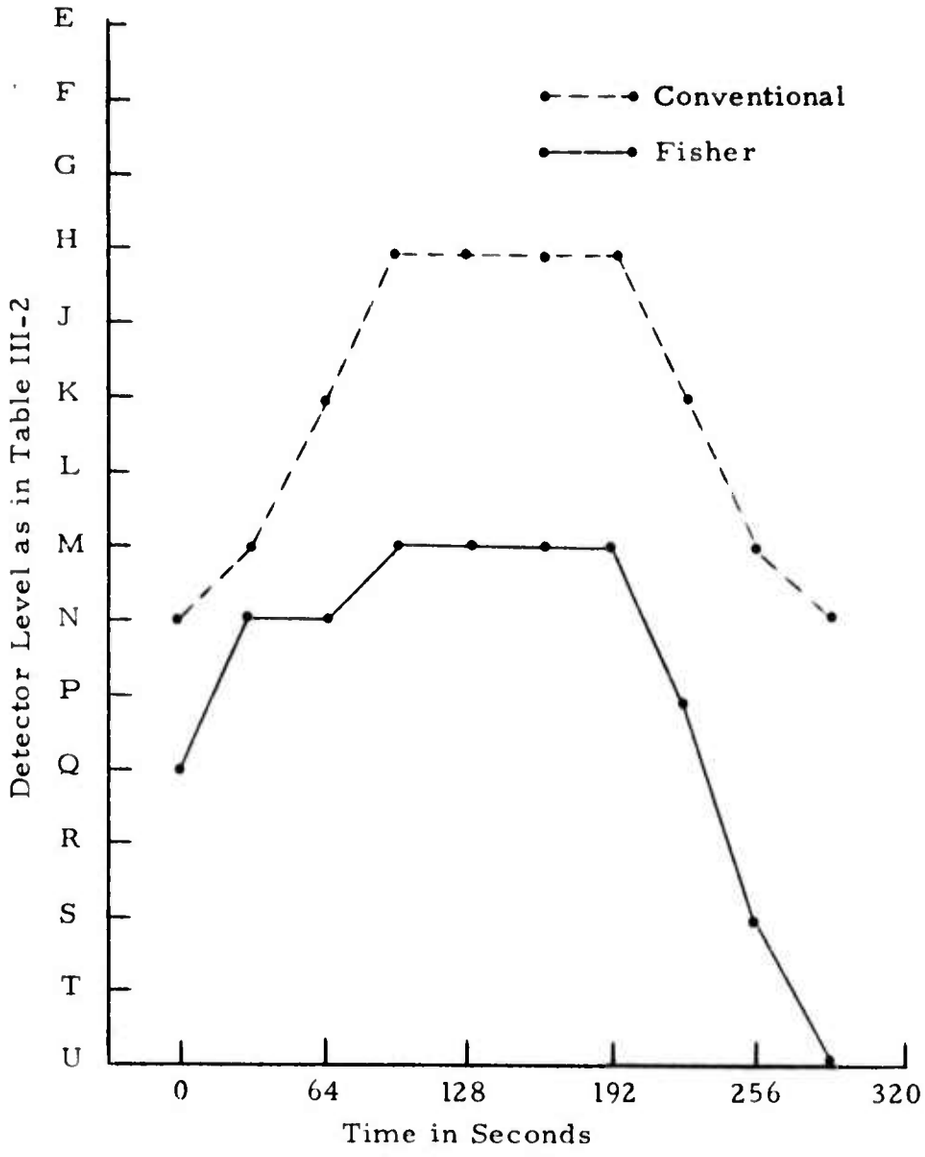

FIGURE III-7

FISHER AND CONVENTIONAL DETECTOR RESPONSE

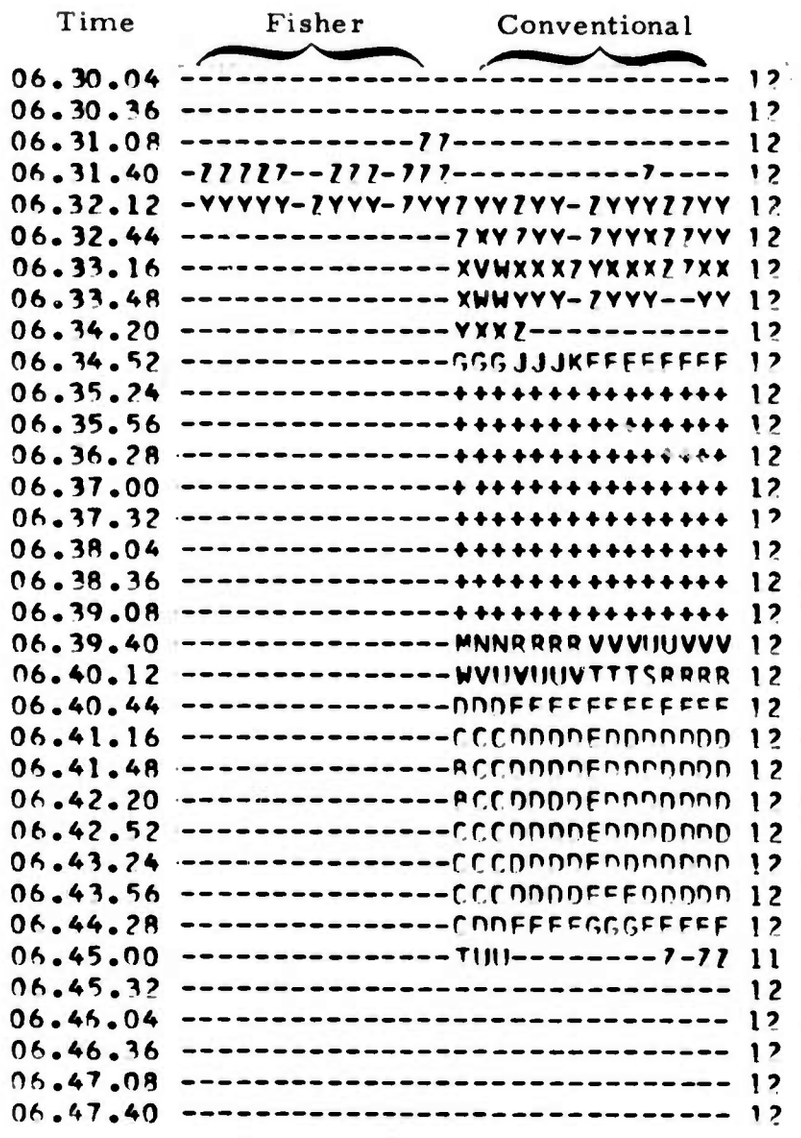

Azimuths Spaced at 15° Intervals About Primary Beam Direction
Detector Level as in Table III-2

FIGURE III-8

RESPONSE OF FISHER AND CONVENTIONAL
DETECTORS TO GLITCH IN DATA

If a signal had been present at the same time as the glitch, the Fisher detector would have missed it. The beam detector will give extra false alarms due to glitches, but these false alarms can be investigated for the presence of signals.

SECTION IV
CONCLUSIONS

A theoretical analysis of the Fisher detector and conventional detector has been carried out, assuming only that the noise is not correlated with itself or the signal. This analysis shows that the Fisher and conventional detectors should respond in the same way to signals and should have the same response to off-azimuth signals. The conventional detector is not sensitive to phase or amplitude distortion, but the Fisher detector output is reduced by phase distortion, although not by amplitude distortion.

Experimental results confirm these predictions. The experimentally determined performance characteristic, an objective measure of how well a detector performs, is the same for the Fisher detector and conventional detector, within the limits imposed by the data sample. The length of time over which the data are averaged has a significant effect. Longer times, up to at least 256 seconds, give better results.

The rejection of off-azimuth signals is the same for the detectors, as predicted. Evidence of saturation due to phase distortion in the Fisher detector was found, and was consistent with the predictions of Section II. The behavior of the detectors in response to glitches in the data was investigated, and the prediction that the Fisher detector does not respond to glitches was confirmed.

One of the difficulties with the conventional beam power detector in the past was that an accurate estimate of the average noise power, σ_o^2, was hard to find. It was anticipated that the Fisher detector would prove superior to the conventional detector because it does not require such an

estimate. The lack of distinction between the detectors found in this study implicitly suggests that the method used to estimate σ_o^2 is a good one.

A number of suggestions for further study can be made. The data base should be expanded, both by investigating more events in the magnitude range of this report, and by taking a wider range of magnitudes. The performance characteristics may be distinguishable if this is done. Longer time gates should be used, as suggested by the results of Section III.

SECTION V
REFERENCES

Alsup, S. A., and E. S. Becker, 1973, Simultaneous Three-Component Broad Band Earth Noise Structure at Very Long Period Experiment Stations, Special Report No. 10, Texas Instruments Incorporated.

Barnard, T. E., 1973, Simulated On-Line Adaptive Processing Results Using Alaska Long Period Array Data, Special Report No. 2, Texas Instruments Incorporated.

Edwards, J. P., III, S. A. Benno, and G. Creasey, 1967, Evaluation of the CPO Auxiliary Processor, CPO Special Report No. 5, Texas Instruments Incorporated.

Strauss, A. C., 1973, Final Evaluation of the Detection and Discrimination Capability of the Alaskan Long Period Array, Special Report No. 8, Texas Instruments Incorporated.

APPENDIX A

CALCULATION OF THE NOISE POWER

A question not addressed in Section II is the calculation of σ_o^2, the noise power. Ideally this power should be calculated over an interval which is known to be free of signals. On the other hand, the noise field changes slowly with time, so a single value for the noise power cannot be used for all time. An attempt is made to satisfy the requirements of continuing adaptation and exclusion of signals in the present detector. Previous work (Barnard, 1973), did not meet these requirements and give rise to unacceptable results.

The data, before being input to either detector, is quality checked for dead or unreasonably large channels. After the beam is formed, in a particular direction, the average noise power for that beam is calculated, over basic time gates of 32 seconds. The logarithms of these powers are taken, and exponentially smoothed into past time. That is, powers at previous times get exponentially less weighting than do powers at recent times.

The logarithm is taken before smoothing because it has been found (Alsup, 1973) that noise power distributions are skewed, in that powers larger than the mean occur more often than half the time. Taking logarithms before smoothing reduces the influence of these powers.

The smoothing process described above is repeated every 32 seconds, so that the average power is updated. Whenever a noise power exceeds the current smoothed average by 6 dB or more, it is assumed that a signal is present, and the updating process is stopped, to be continued after the signal has passed. In this way, long term drifts in the noise power are allowed, but signals are not included in the noise power estimate.